Journal of Luminescence 131 (2011) 2473–2477

Contents lists available at ScienceDirect

Journal of Luminescence

journal homepage: www.elsevier.com/locate/jlumin

Synthesis, characterization and optical spectroscopy of Eu^{3+} doped titanate nanotubes

P. Haro-González [a,*], M. Pedroni [b], F. Piccinelli [b], L.L. Martín [a], S. Polizzi [c], M. Giarola [d], G. Mariotto [d], A. Speghini [b], M. Bettinelli [b], I.R. Martín [a]

[a] Departamento de Física Fundamental y Experimental, Electrónica y Sistemas, Universidad de La Laguna, Av. Astrofísico Francisco Sánchez, s/n, 38206, La Laguna, Spain
[b] Laboratorio di Chimica dello Stato Solido, DB, Università di Verona and INSTM, UdR Verona, Ca' Vignal, Strada Le Grazie 15, I-37134 Verona, Italy
[c] Dipartimento di Chimica Molecolare e Nanosistemi, Università Ca' Foscari Venezia and INSTM, UdR Venezia, Via Torino 155/b, 30172, Venezia–Mestre, Italy
[d] Dipartimento di Informatica, Università di Verona Ca' Vignal, Strada Le Grazie 15, I-37134 Verona, Italy

ARTICLE INFO

Article history:
Received 27 April 2011
Received in revised form
13 June 2011
Accepted 15 June 2011
Available online 22 June 2011

Keywords:
Titania nanotubes
Eu^{3+}
Optical spectroscopy

ABSTRACT

The synthesis of Eu^{3+} doped titania nanotubes was carried out via a hydrothermal method. X-ray diffraction and transmission electron microscope analyses showed that the nanotubes were formed by rolling multilayered titania structure with a length of up to 100 nm. The Eu^{3+}-doped nanotubes exhibited strong emission lines associated with the $^5D_0 \rightarrow {}^7F_J$ (with J from 1 to 4) transition of Eu^{3+} and the differences between the luminescence properties of the precursor powders and the nanotubes were studied at low temperature.

1. Introduction

Since their discovery of two decades ago [1], carbon nanotubes have attracted a lot of interest from the scientific community for their unique properties [2]. The different chemical and physical properties of these materials have been ascribed to their characteristic structural features, that is, high surface-to-volume ratios and size-dependent properties. The controlled manipulation of low-dimensional forms has generated much interest in the literature [3], especially nanotubes generated from TiO_2, which have been expected to be applicable such as photocatalysts [4,5], sensors [6], electrochemical capacitors [7], proton conduction [8] and lithium-inserting and ion-exchange materials [9]. Moreover, several studies revealed that titania is a good candidate to be used as host material for the rare-earth (RE) ions to prepare photoluminescent materials [10–13].

Through the years, the luminescence properties of RE ions hosted in several crystalline and non-crystalline matrices such as metal oxides and fluorides, organic complexes and a variety of semiconductors materials have been studied due to their many technological applications [14–17]. As it is known, the luminescence properties of the RE doped host depend critically on their localizations in the host. In this sense, Eu^{3+} ions are widely used as a crystal field probe to test the ion–ion and ion–host interactions [14,18–20]. The main advantages are the simplicity of its energy level structure, the sensitivity shown by the luminescence to the local surroundings and the fact that the $^5D_0 \leftrightarrow {}^7F_0$ transition occurs between non-degenerate levels.

In this work, Eu^{3+} doped titania nanotubes were synthesized by a hydrothermal process where the precursor powder was obtained by the sol–gel. The luminescence spectroscopy of nanotubes was measured and compared with the precursor powder at 10 K. The existence of multiple sites for Eu^{3+} ions was found in the material under investigation.

2. Experimental

2.1. Synthesis of materials

The preparation method of Eu^{3+} doped TiO_2 nanopowders is similar to the classical sol–gel procedure. First, 0.464 mol of $Eu(NO_3)_3 \cdot 5\ H_2O$ were dissolved in 44.8 ml of 2-propanol and then 6.9 ml of acetylacetone were added. After a few minutes of vigorous stirring 2.3 mol of titanium isopropoxide was added and finally 5 ml of citric acid aqueous solution (1% wt). The resultant solution was maintained under vigorous stirring for 5–6 h and was dried at RT for 24 h. The obtained gel was heated at 500 °C for 24 h and the resulted powder was collected.

Titania Eu^{3+} doped nanotubes were synthesized by a classical hydrothermal method similar to the method developed by

* Corresponding author. Tel.: +34922318651.
E-mail address: patharo@ull.es (P. Haro-González).

0022-2313/$ - see front matter © 2011 Elsevier B.V. All rights reserved.
doi:10.1016/j.jlumin.2011.06.029

Morgan et al. [3] for TiO_2 undoped nanotubes. First, 0.150 g of the powder previously obtained was mixed with 80 ml of NaOH 10 M [21] and then transferred into a teflon vessel where heated at 120 °C for 72 h. After cooling to room temperature the powder was washed several time with HCl 0.1 M and deionized water until the pH was less than 7 and separated from the solution by centrifugation. Finally the nanotubes were collected and dried at room temperature for one day.

2.2. Measurements

X-Ray powder diffraction (XRPD) data were taken with a Thermo ARL X'TRA powder diffractometer, operating in the Bragg–Brentano geometry equipped with a Cu-anode X-Ray source (K_α, $\lambda = 1.5418$ Å) and using a Peltier Si(Li) cooled solid state detector. The patterns were collected with a scan rate of 0.04 °/s, with measurement times of 1.0 s/step and a 2θ range of 5°–90°. The phase identification was performed with the PDF-4+ 2009 database provided by the International Center for Diffraction Data (ICDD). The samples were carefully homogenized in a mortar, suspended in a few drops of ethanol and deposited in a low-background sample stage. Before starting the pattern collection the ethanol was completely evaporated.

The room temperature Raman spectrum was obtained upon the 568.2 nm excitation line of an Ar^+/Kr^+ mixed-gas ion laser and detected by a CCD, with 1024×256 pixels, cryogenically cooled by liquid nitrogen. The laser beam was focused onto the sample surface, with a spot size of about 2 mm, by a 100X objective with N.A. = 0.9. The Stokes component of the backscattered radiation was analyzed by a triple-monochromator spectrometer (Horiba-Jobin Yvon, model T64000), operated in double-subtractive/single configuration, and equipped with three 1800 grooves/mm gratings, which ensured a spectral resolution better than 1 cm^{-1}/pixel over the whole scanned spectral range.

Luminescence measurements were carried out upon excitation with a tunable dye laser pumped by Nd:YAG laser. For low temperature measurements, the samples were mounted on a closed cycle He cryostat. The emission signal was analyzed by a half-meter monochromator (HR460, Jobin Yvon) equipped with a 1200 lines/mm grating and detected with a CCD detector (Spectrum One, Jobin Yvon) or with a photomultiplier. The spectral resolution of the emission spectra is 0.1 nm.

3. Results and discussion

3.1. Structural and morphological characterization

The composition of the Eu^{3+} doped nanocrystalline titania starting powder used to synthesize the titanate nanotubes was found to be anatase (62%, volume fraction) and rutile (38%, volume fraction) (Fig. 1.a) [22]. The hydrothermal treatment on this powder leads to the formation of titanate nanotubes as evidenced by the comparison between the measured XRPD patterns (Fig. 1.b) and the powder patterns reported previously for titanate nanotubes [8,23–25], and by the comparison with the PDF reference card number 00–047–0124 for titanate with $H_2Ti_2O_5 \cdot H_2O$ stoichiometry (vertical lines, Fig. 1). Worth to be mentioned is the characteristic broad peak at 2θ closes to 10° attributed to the interlayer diffraction of the titanate nanotubes. In the present case, the 2θ position of this peak is slight shifted compared to the one present in $H_2Ti_2O_5 \cdot H_2O$, reflecting a different d spacing of this family of lattice planes (Fig. 1). The addition of 2 mol% (nominal) Eu^{3+} in the host is not expected to produce any observable change in the powder X-ray diffraction pattern of the undoped host.

The room temperature Raman spectrum is shown in Fig. 2. The spectrum consists of several Raman bands partly overlapped, due to the intrinsic disordered nature of the material under investigation, compatible with the broad diffraction peaks observed in the XRPD pattern. A straightforward assignment of all the observed bands is therefore a hard task. Characteristic bands typically assigned to titanate nanotubes are observed in the spectrum at Raman shifts of 196, 276, 446, 657, 698 and 900 cm^{-1}. The relative intensities and the widths of the bands are quite similar to those observed for titanate nanotubes, with pseudolepidrocite layer structure, reported by other authors [26,27]. In particular, the strong and broad band peaked at 276 cm^{-1} can be assumed as a key indicator of the formation of the nanotube phase, as pointed out by Morgan et al. [28]. In our case, an additional, quite narrow, band peaked at 144 cm^{-1} is attributed to the E_g vibrational mode of anatase TiO_2 [29], present as a segregated phase. Nonetheless, the amount of the TiO_2 very low, most probably lower than 2% in

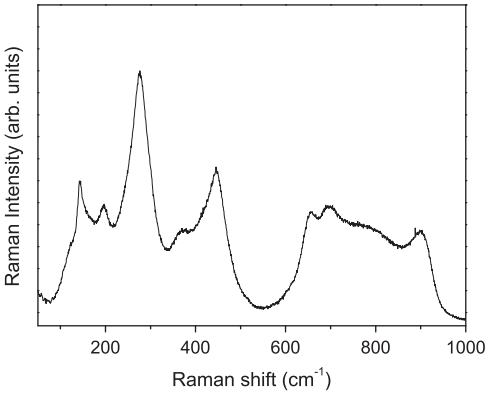

Fig. 2. Room temperature Raman spectrum of the titanate nanotubes.

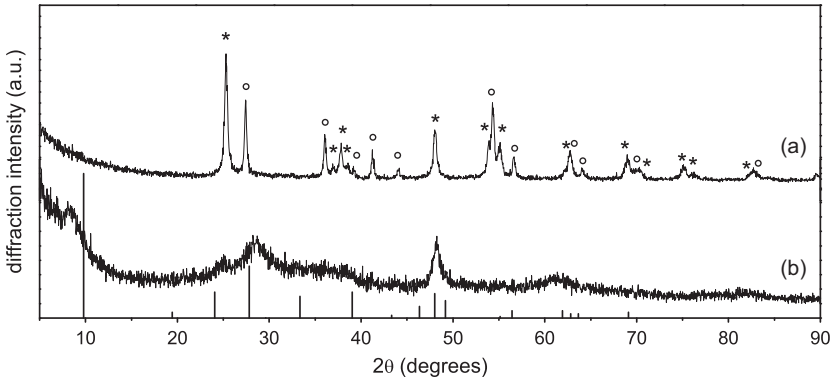

Fig. 1. XRPD patterns of the starting Eu^{3+} doped titania powder (a), where (*) gives anatase and (°) rutile phase, and the obtained titanates nanotubes (b) together with the reference PDF card for $H_2Ti_2O_5 \cdot H_2O$ (vertical lines).

weight, as evidenced from a recent Raman investigation [30], in agreement to the absence of any diffraction peak due to crystalline TiO_2 phase in the measured X-Ray diffraction powder patterns of the present nanotubes. Again, the small nominal doping level is not expected to give rise to any observable change in the Raman spectrum of the undoped host.

Fig. 3 shows TEM micrographs of the Eu^{3+} doped final material where nanotubes with a length of up to 100 nm are observed. The HRTEM image in Fig. 4 suggests the presence of a different number of walls on opposite sides of the nanotube, further suggesting the scroll-like structure. These multiwall-structured nanotubes have an outer diameter of 7 nm and inner pore diameter of 2 nm with interlayer spacing of 0.7 nm.

3.2. Luminescence properties

Emission spectra were measured on nanotubes and on precursor powders upon excitation the $^5D_0$ level of Eu^{3+} at 520 nm (see Fig. 5). The Eu^{3+}: $^5D_0 \rightarrow {}^7F_J$ (with J from 1 to 4) transitions were clearly appreciated at 10 K. Only emission from the first level $^5D_0$ of the ^5D_J multiplet was observed, revealing that high-energy lattice vibrations make the multi-phonon relaxation process predominant from the $^5D_1$ level. The red emission centered at 612 nm was due to the forced electric dipole transition ($^5D_0 \rightarrow {}^7F_2$), which was allowed on condition that the Eu^{3+} ion occupied a site without an inverse center [14,18]. This transition is highly sensitive to structural changes and environmental effects in the vicinity of the Eu^{3+} ion. The peaks near 590 nm were derived from the allowed magnetic dipole transition ($^5D_0 \rightarrow {}^7F_1$). Peaks at 580, 655 and 700 nm were attributed to the $^5D_0 \rightarrow {}^7F_0$, $^5D_0 \rightarrow {}^7F_3$ and $^5D_0 \rightarrow {}^7F_4$ transitions, respectively. In agreement with previous results [19,20], it is expected luminescence spectra characterized by inhomogeneously broadened bands, typical of Eu^{3+} doped disordered system. As can be seen, the emission spectrum of the Eu^{3+}-doped nanotubes (Fig. 5.b) shows different luminescence properties compared with the precursor powders (Fig. 5.a). The peak sites are similar whereas the emission shapes are more resolved for the nanotube sample.

Decays of the luminescence of the $^5D_0$ level were measured on nanotubes and on precursor powders upon excitation at 520 nm at 10 K (see Fig. 6). At this excitation wavelength, it is expected to obtain luminescence from all the Eu^{3+} sites, which could explain a non-exponential behavior. In order to compare different curves, it is useful to evaluate an average lifetime with the following equation:

$$\tau = \frac{\int_0^\infty I(t)tdt}{\int_0^\infty I(t)dt} \quad (1)$$

Values of 688 and 382 μs were found for the nanotubes and the precursor powder, respectively. At low temperature, the fluorescence decay of the Eu^{3+}: $^5D_0$ state is entirely due to radiative transitions. This follows from the fact that at room temperature the fluorescence lifetime decreases by only a few percent relative to its value at 10 K. Thus the room temperature fluorescence lifetime is almost entirely due to radiative relaxation; non-radiative decay processes are still not significant.

The lifetime in nanotubes is significantly longer than the lifetime in the precursor powder. One possible explanation could be given in the term of different asymmetry of the coordination of the Eu^{3+} ions between the titania nanotubes and titania powders [20]. It is well known that the asymmetry ratio R, of the integrated intensities of the $^5D_0 \rightarrow {}^7F_2$ and $^5D_0 \rightarrow {}^7F_1$ can be considered indicative of the asymmetry, given by

$$R = \frac{I(^5D_0 \rightarrow {}^7F_2)}{I(^5D_0 \rightarrow {}^7F_1)} \quad (2)$$

The lower R value shows the higher symmetry site of the Eu^{3+} ions. From the emission spectra (see Fig. 5), the value of the asymmetry parameter was obtained and results to be 4.8 on the precursor powder and 5.4 on nanotubes. The two values appear to be comparable and another explanation is therefore necessary. The lengthening of the emission decay time to the $^5D_0$ level can be due to a lower effective refractive index surrounding the Eu^{3+} ion in the nanotubes with respect to the precursor powder, due to the fact that the filling factor is lower than one as evidenced also for other Eu^{3+} doped nanocrystalline materials [31].

The emission spectra at 10 K were measured in the range of the $^5D_0 \rightarrow {}^7F_0$ transition on the nanotubes and on the precursor powders (see Fig. 7). Multiple sites are expected for trivalent Eu^{3+} ions because of charge imbalance. For the precursor powder, the emission spectrum revealed at least three nonequivalent sites of

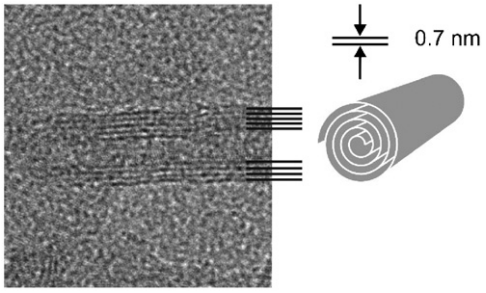

Fig. 4. HRTEM image showing the wall structure of a nanotube.

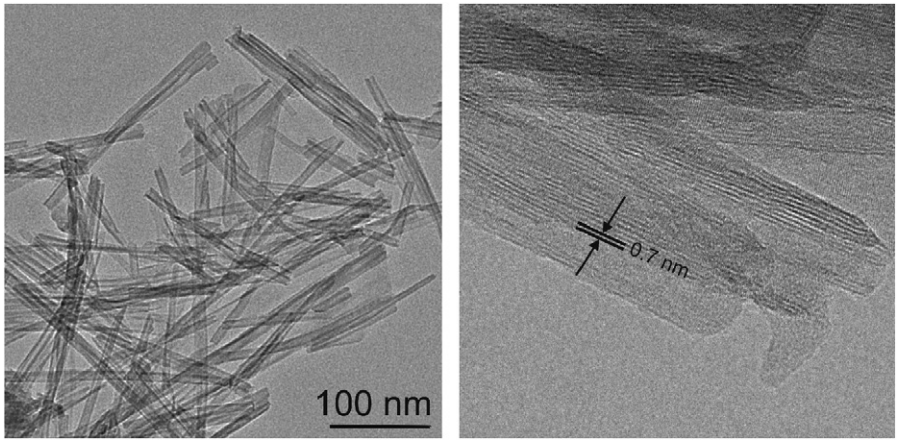

Fig. 3. TEM image of Eu^{3+} doped nanotubes.

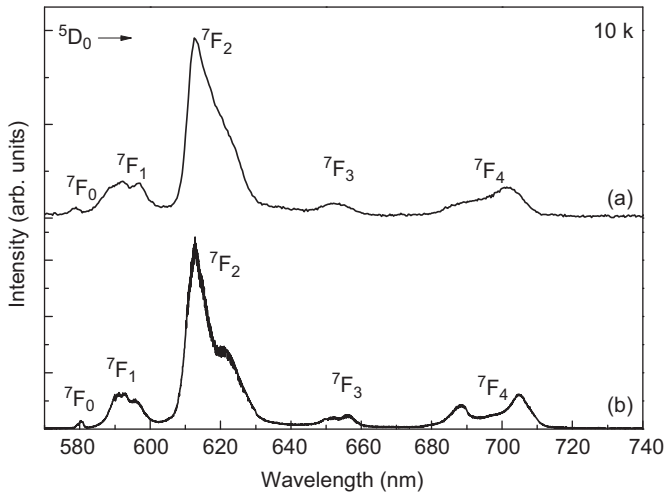

Fig. 5. Emission spectra for the Eu^{3+} doped titania powder (a) and nanotubes (b) obtained at 10 K.

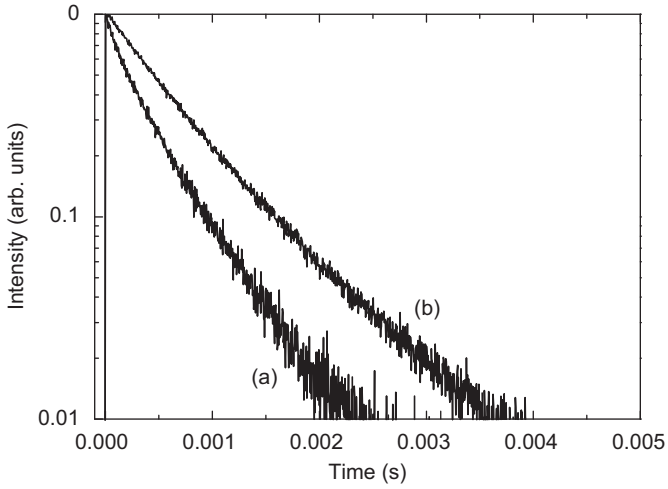

Fig. 6. Decay of the luminescence for the $^5D_0$ level of the Eu^{3+} ions at 10 K for the titania powder (a) and nanotubes (b).

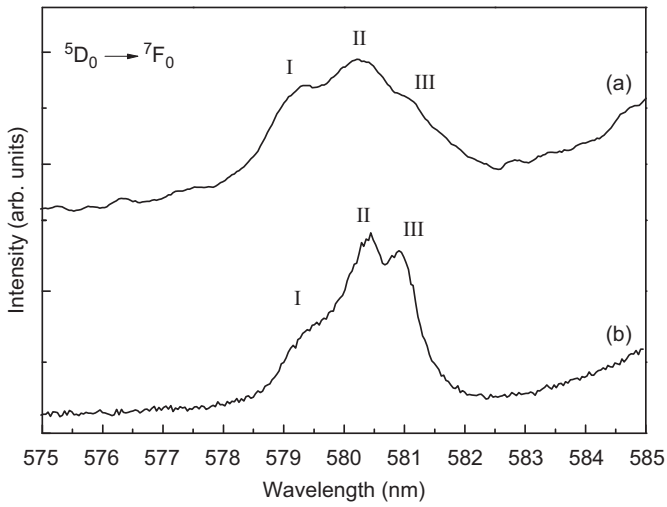

Fig. 7. Emission spectra for the Eu^{3+}: $^5D_0 \rightarrow {}^7F_0$ transition recorded at 10 K for the titania powder (a) and nanotubes (b).

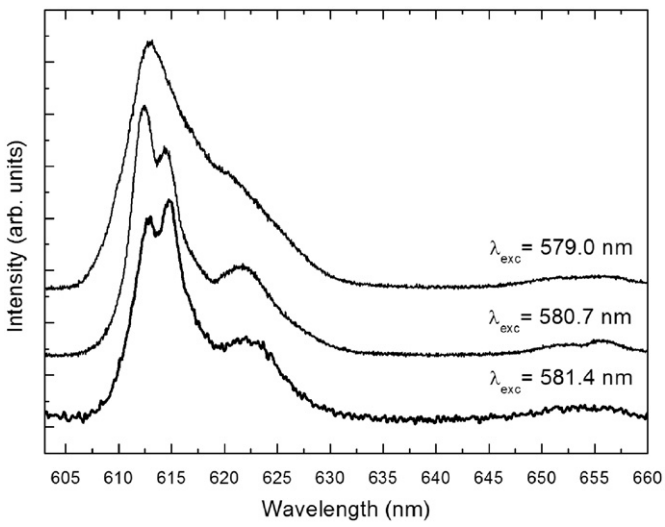

Fig. 8. Emission spectra for the Eu^{3+}: $^5D_0 \rightarrow {}^7F_2$ transition recorded at 10 K for the titania nanotubes under excitation at 579, 580.7 and 581.4 nm.

Eu^{3+} ions. Luo et al. [14] reported the incorporation of Eu^{3+} ions in anatase TiO_2 nanocrystals via the sol–gel where three nonequivalent sites of Eu^{3+} were found in good agreement with our result. Moreover, the emission spectrum for the nanotubes revealed three nonequivalent sites of Eu^{3+} ion, where, in this case, the observation of these sites is clearer than for the precursor powder. This spectrum shows a strong overlap for these sites confirming the high disorder of the crystalline environment of the Eu^{3+} ions in the TiO_2 host [14,19–20]. The presence of such disorder is ascribed to the significant difference in the ionic radii in octahedral coordination for Ti^{4+} (74.5 pm) and Eu^{3+} (108.7 pm) ions [13,19], so the substitution of the dopant ion cannot easily occur without distortions, which could be affected by a site-to-site variation.

During the formation of nanotubes, it is possible for the Eu^{3+} ions to enter the interstitial cavities between the layers in the nanotubes wall due to the small interlayer distance of the nanotubes, 0.7 nm, which is much higher than the Eu^{3+} ionic radio. The possible sites for Eu^{3+} in titania nanotubes are limited to the interlayer space and inner surface of the nanotubes.

Finally, emission spectra at 10 K were obtained for the $^5D_0 \rightarrow {}^7F_2$ transition in nanotubes sample at three different excitation wavelengths (see Fig. 8). This excitation was carried out at the possible three nonequivalent sites of the Eu^{3+} ions according to the $^5D_0 \rightarrow {}^7F_0$ transition. The high sensitivity to structural and environmental changes of this transition gives rise the small differences in Fig. 8.

4. Conclusions

The synthesis of Eu^{3+} doped titania nanotubes was carried out successfully via a hydrothermal treatment method from a precursor powder. The differences between the precursor powder and the nanotubes were studied by X-ray powder diffraction, Raman spectroscopy, transmission electron microscope technique and optical spectroscopy. These results showed the formation of Eu^{3+}-doped titanate nanotubes constructed by rolling multilayered titania structure concentrically arranged with a length of up to 100 nm. The luminescence spectra of the precursor powders and of the nanotubes revealed a strong emission lines associated to the $^5D_0 \rightarrow {}^7F_J$ transition of the Eu^{3+} ions, where at least three nonequivalent sites were found for the Eu^{3+} ions.

Acknowledgments

The authors are grateful to Fondazione Cariverona (Verona, Italy), Comisión Interministerial de Ciencia y Tecnología (MAT2010-21270-C04-02), Malta Consolider Ingenio 2010 (CSD2007-0045) and FPI of Gobierno de Canarias for financial support.

References

[1] S. Iijima, Nature 354 (1991) 56.
[2] M.S. Dresselhaus, P. Avouris, Carbon Nanotubes: Synthesis, Structure, Properties and Applications, Springer, Heidelberg, 2001.
[3] D.L. Morgan, Huai-Yong Zhu, Ray L. Frost, Eric R. Waclawik, Chem. Mater. 20 (12) (2008) 3800.
[4] M. Adachi, Y. Murata, M. Harada, S. Yoshikawa, Chem. Lett. 29 (2000) 942.
[5] T. Kubo, M. Takeuchi, M. Matsuoka, M. Anpo, A. Nakahira, Catal. Lett. 130 (2009) 28.
[6] S. Liu, A. Chen, Langmuir 21 (2005) 8409.
[7] Y.G. Wang, X.G. Zhang, J. Electrochem. Soc. 152 (2005) A671.
[8] A. Thorne, A. Kruth, D. Tunstall, J.T.S. Irvine, W. Zhou, J. Phys. Chem. B 109 (2005) 5439.
[9] H. Zhang, G.R. Li, L.P. An, T.Y. Yan, X.P. Gao, H.Y. Zhu, J. Phys. Chem. C 111 (2007) 6143.
[10] A. Conde-Gallardo, M. Garcia-Rocha, I. Hernandez-Calderon, R. Palomino-Merino, Appl. Phys. Lett. 78 (2001) 3436.
[11] S. Jeon, P.V. Braun, Chem. Mater. 15 (2003) 1256.
[12] R. Asahi, T. Morikawa, T. Ohwaki, A. Aoki, Y. Taga, Science 293 (2001) 269.
[13] B. Chi, E.S. Victorio, T. Jin, Nanotechnology 17 (2006) 2234.
[14] W. Luo, R. Li, G. Lui, M.R. Antonio, X. Chen, J. Phys. Chem. C 112 (28) (2008) 10370.
[15] P. Haro-González, F. Lahoz, J. González-Platas, J.M. Cáceres, S. González-Pérez, D. Marreno-López, N. Capuj, I.R. Martín, J. Lumin. 128 (2008) 908.
[16] P. Haro-González, I.R. Martín, E. Arbelo-Jorge, S. González-Pérez, J.M. Cáceres, P. Núñez, J. Appl. Phys. 104 (2008) 013112.
[17] P. Haro-González, I.R. Martín, Albero Hernandez Creus, Opt. Express 18 (2) (2010) 582.
[18] J. Méndez-Ramos, V. Lavín, I.R. Martín, U.R. Rodríguez-Mendoza, V.D. Rodríguez, A.D. Lozano-Gorrín, P. Núñez, J. Appl. Phys. 94 (4) (2003) 2295.
[19] M. Bettinelli, A. Speghini, D. Falcomer, M. Daldosso, V. Dallacasa, L. Romanò, J. Phys.: Condens. Matter 18 (2006) S2149.
[20] P. Ghigna, A. Speghini, M. Bettinelli, J. Solid State Chem. 180 (2007) 3296.
[21] T. Kasuga, M. Hiramatsu, A. Hoson, T. Sekino, K. Niihara, Adv. Mat. 11 (1999) 1307.
[22] L. Lutterotti, S. Gialanella, Acta Mater. 46 (1997) 101.
[23] G.H. Du, Q. Chen, R.C. Che, Z.Y. Yuan, L.-M. Peng, Appl. Phys. Lett. 79 (2001) 79.
[24] S. Zhang, L.-M. Peng, Q. Chen, G.H. Du, G. Dawson, W.Z. Zhou, Phys. Rev. Lett. 91 (2003) 256103.
[25] C.C. Tsai, H. Teng, Chem. Mater. 18 (2006) 367.
[26] T. Beuvier, M. Richard-Plouet, L. Brohan, J. Phys. Chem. C 114 (2010) 7660.
[27] T. Gao, H. Fjellvag, P. Norby, J. Phys. Chem. B 112 (2008) 9400.
[28] D.L. Morgan, H.-W. Liu, R.L. Frost, E.R. Waclawik, J. Phys. Chem. C 114 (2010) 101.
[29] M. Giarola, A. Sanson, F. Monti, G. Mariotto, M. Bettinelli, A. Speghini, G. Salviulo, Phys. Rev. B (81) (2010) n. 174305.
[30] S.-J. Kim, Y.-U. Yun, H.-J. Oh, S.H. Hong, C.A. Roberts, K. Routray, I. Wachs, J. Phys. Chem. Lett. 1 (2010) 130.
[31] R.S. Meltzer, S.P. Feofilov, B. Tissue, H.B. Yuan, Phys. Rev. B 60 (20) (1999) R14012.